Biophysical Journal Volume 67 October 1994 1620–1633

Oblique Section 3-D Reconstruction of Relaxed Insect Flight Muscle Reveals the Cross-Bridge Lattice in Helical Registration

Holger Schmitz, Carmen Lucaveche, Michael K. Reedy, and Kenneth A. Taylor
Department of Cell Biology, Duke University Medical Center, Durham, North Carolina 27710 USA

ABSTRACT In this work we examined the arrangement of cross-bridges on the surface of myosin filaments in the A-band of *Lethocerus* flight muscle. Muscle fibers were fixed using the tannic-acid-uranyl-acetate, ("TAURAC") procedure. This new procedure provides remarkably good preservation of native features in relaxed insect flight muscle. We computed 3-D reconstructions from single images of oblique transverse sections. The reconstructions reveal a square profile of the averaged myosin filaments in cross section view, resulting from the symmetrical arrangement of four pairs of myosin heads in each 14.5-nm repeat along the filament. The square profiles form a very regular right-handed helical arrangement along the surface of the myosin filament. Furthermore, TAURAC fixation traps a near complete 38.7 nm labeling of the thin filaments in relaxed muscle marking the left-handed helix of actin targets surrounding the thick filaments. These features observed in an averaged reconstruction encompassing nearly an entire myofibril indicate that the myosin heads, even in relaxed muscle, are in excellent helical register in the A-band.

INTRODUCTION

Muscle contraction is widely believed to occur through an active sliding motion of thick myosin filaments and thin actin filaments, mediated by an ATP-driven cyclical attachment of myosin cross-bridges to the thin filaments (Huxley, 1957). The recently published x-ray crystal structure of the major components of the contractile cycle, myosin subfragment 1 (Rayment et al., 1993), and actin (Holmes et al., 1990) has brought within reach an understanding of these molecular interactions at the atomic level. Ultimately, the process of force production in muscle must be understood at the level of the sarcomere itself, where lattice structure governs the distribution of cross-bridges and cross-bridge states during muscle contraction, and where a series of weakly bound states of myosin and actin lead up to the strongly bound actomyosin states that comprise the power stroke. Formation of weakly bound cross-bridges that occur at the beginning of the power stroke is expected to be heavily influenced by lattice constraints.

Insect flight muscles (IFM) from the large waterbug *Lethocerus* sp. have been widely used in the study of cross-bridge structure in situ because of their highly ordered and regular construction. Both x-ray diffraction (M. K. Reedy et al., 1965; Miller and Tregear, 1972; Holmes et al., 1980; Tregear et al., 1990) and 3-D electron microscopy (Taylor et al., 1984, 1989a, b, 1993) have been applied to the study of cross-bridges in situ. Studies using 3-D electron microscopy have demonstrated lattice effects even in rigor muscle, where 20% of myosin heads do not attach to actin and where single- and double-headed cross-bridges reveal a range of tilt angles. In rigor muscle, the thin filament arrangement has a strong influence on cross-bridge formation, because the strong affinity of nucleotide-free myosin heads for actin can overcome to some extent the geometrical influence of the thick filament origins. However, in more weakly bound cross-bridge states, the thick filament origin of myosin heads will exert a relatively stronger influence on the location of cross-bridges.

Despite the apparently near-crystalline order of IFM, there is evidence for disorder in both the thick and thin filament arrangements. Thin filaments in IFM have a helical structure of 28 subunits in 13 turns of the left-handed genetic helix and a pitch of 38.7 nm that matches the most pronounced thick filament layer line spacing. They are positioned in the lattice at dyad or pseudo-dyad positions between pairs of thick filaments. In their description of the x-ray diffraction pattern of rigor IFM, Holmes et al. (1980) suggested that the thin filaments have a random 180° rotational disorder throughout the filament lattice. However, Wray et al. (1979) found x-ray evidence for a more regular arrangement of the thin filament lattice lacking this rotational disorder. This disorder would have a relatively subtle effect on the cross-bridge arrangement because of the thin filament positions in the unit cell. Thus, only one x-ray layer line and no EMs can as yet detect the <3-nm difference between cross-bridge labeling of thin filaments that distinguishes two alternative symmetries of the actin filament position in the unit cell. However, at 5–10 nm resolution, actin target lattice ordering (the axial and rotational ordering of thin filaments) is very stably maintained, thereby supporting a very well aligned rigor cross-bridge lattice across the fibril even when thick filaments obviously wander in axial register by several tens of nanometers across the same sarcomere.

The thick filament structure and azimuthal positioning within the filament lattice has been more difficult to determine. Thick filaments in rigor show a twofold flared-X formation that distributes four cross-bridges at each level. This

Received for publication 20 December 1993 and in final form 31 May 1994.

Address reprint requests to Dr. Holger Schmitz, Department of Cell Biology, Duke University Med. Ctr., Durham, NC 27710. Tel.: 919-684-4702; Fax: 919-684-3687; E-mail: holger@marimba.cellbio.duke.edu.

Abbreviations used: IFM, insect flight muscle; CSSR, crystallographic serial section reconstruction; 2-D, 3-D, two-, three-dimensional; EM, electron micrograph; TnH, troponin-H.

0006-3495/94/10/1620/14 $2.00

structure repeats every 12.9 nm axially with a 60° rotation so that it follows and marks the two-start, left-handed helix of actin target zones (Reedy and Reedy, 1985; Taylor et al., 1993). (Target zones are 10–15 nm segments in each 38.7 nm helix repeat where the azimuth of actin subunits is sterically best positioned to receive cross-bridges from an adjacent thick filament.) The early conflict between flared-X appearances suggesting two myosins per 13–15 nm versus mass and protein quantification that indicated six myosins per repeat was relieved when modeling showed that strong rigor interactions with the actin target lattice could produce the flared X while hiding the inherent symmetry and periodicity of thick filaments (Squire, 1972; Offer and Elliott, 1978; Haselgrove and Reedy, 1984). Thus, the twofold flared X was no obstacle when inherent fourfold symmetry of *Lethocerus* IFM thick filaments was first suggested by Wray's (1979b) models of myosin packing in the filament backbone. Confirming evidence by mass/length measurement (M. K. Reedy et al., 1981) and 3-D reconstruction (Morris et al., 1991) from individual relaxed thick filaments led to the current model, where four myosins—eight heads—project with fourfold symmetry at every 14.5 nm axial repeat or crown. This was first visualized in situ with fibers fixed by a new procedure dubbed "TAURAC" (M. K. Reedy et al., 1991), from which thin cross sections show clear tetragonal crowns and longitudinal sections show the right-handed 38.7 nm helical repeat of thick filaments in a way clearly distinguishable from the left-handed 38.7 nm helix repeat of the actin target lattice (M. K. Reedy et al., 1992, 1993).

Several types of thick filament disorder have been observed in IFM. Freundlich and Squire (1983) analyzed relaxed and rigor *Lethocerus* M-band structure, where the myosin filaments appear elliptical in cross section. They observed apparently three different filament orientations 60° apart but distributed across the lattice in a random biased fashion. Based on this observation, they concluded that the filaments will express the same randomized rotational orientation into the A-band. Because it is known that *Lethocerus* myosin filaments are four-stranded, with four pairs of heads per crown azimuthally separated by 90° (Wray, 1979b; Morris et al., 1991), a random 60° azimuthal disorder of the thick filaments would result in a disordered arrangement of unattached cross-bridges in the A-band. The M-band of *Lethocerus* flight muscle is poorly ordered compared with that of other species, e.g., *Apis* (Honeybee), so that disorder in the A-band is expected. However, *Apis* flight muscle has a very well ordered M-band (Auber, 1967), so that correlation of its A-band disorder (Schmitz et al., 1994) with the M-band order would be unexpected.

More recently, thorough investigation of the structure and arrangement of myosin filament backbones in *Apis*, *Phormia* (Fleshfly), *Musca* (Housefly), and *Lethocerus* (Beinbrech et al., 1988, 1990; Schmitz et al., 1994) revealed a different sort of disorder. In contrast to Wray's model, which predicts a helical arrangement of 12 symmetrical subfilaments in the myosin filament backbone, these studies revealed a set of six pairs of subfilaments that run parallel to the long filament axis (Schmitz et al., 1993). Analysis of the rotational orientation of the myosin backbones of *Musca*, *Apis*, *Lethocerus*, and *Phormia* indicates that, with respect to axial rotation, the thick filaments and, therefore, the cross-bridges that originate from the backbone, are randomly oriented in the A-band (Beinbrech et al., 1990; Schmitz et al., 1994). This random orientation of myosin filament backbones is a more fundamental type of disorder than that observed by Freundlich and Squire (1983) because it would result in random cross-bridge azimuths in the A-band irrespective of 60° azimuthal disordering.

These types of A-band disorder run contrary to observations of the very regular arrangement of cross-bridges in IFM under several different conditions. In rigor, the very regular arrangement of cross-bridges has been assumed to be a result of a regular lattice of actin targets. However, a visible variation of cross-bridges marking a regular 116 nm axial repeat can be seen in rigor EMs (M. K. Reedy, 1968; Haselgrove and Reedy 1978; Reedy and Reedy, 1985) and 3-D reconstructions (Taylor et al., 1993) as well as in EMs of IFM states with bound nucleotide (M. C. Reedy et al., 1987; M. K. Reedy et al., 1992, 1993). This observation requires both lateral and close rotational register among adjacent thick filaments across the entire sarcomere, or else the 116-nm repeat would be axially randomized on either side of the actin filaments. The 116-nm repeat is not only an axial vernier of 14.5 nm against 38.7 nm, but is also an azimuthal vernier of the 60° rotation of the hexagonal lattice against a 67.5° rotation ($2 \times 33.75°$) that arises from the helical pitch of cross-bridges on the thick filament surface. The match of this vernier on adjacent filaments is a necessity for making visible the expression of 116 nm in cross-bridge attachment frequency in EMs, and in turn requires rotational alignment among the adjacent thick filaments.

In this work we examined the arrangement of the cross-bridges in the A-band on the surface of myosin filaments of TAURAC-fixed, relaxed *Lethocerus* flight muscle. This new fixation procedure preserves the helical arrangement of the cross-bridges remarkably well, providing a unique opportunity to investigate muscle structure in a nonrigor state reasonably close to that of relaxed muscle. The 3-D reconstruction reveals that, despite the intrinsic disorders previously observed in this muscle, the cross-bridges on the surface of relaxed IFM are arranged in excellent helical register. The apparently conflicting observations of ordered cross-bridges and disordered backbones can be reconciled by a new model for the thick filament arrangement in *Lethocerus* flight muscle.

MATERIALS AND METHODS

Specimen preparation and electron microscopy

Dorsal longitudinal flight muscles of *Lethocerus indicus* glycerinated in relaxing buffer were used for this work. The fibers used in this study had not been rigorized. Single fibers were mounted on U pins (M. C. Reedy et al., 1994) and fixed using the TAURAC tannic-acid-uranyl-acetate procedure (M. K. Reedy et al., 1991), first in 0.2% tannic acid in relaxing buffer for 30 min on ice, then after five rinses in deionized water were post-fixed in uranyl acetate for 30 min before routine ethanol dehydration and Araldite embedding as described (M. C. Reedy et al., 1983). Very dark gray to nearly

black sections were cut and collected for microscopy. We judge the section thickness to be about 15 nm, based on the clear visibility of cross-bridges and the observation of occasional section folds in EMs. Micrographs were obtained at magnifications of 20,000X on a Siemens 101 electron microscope operated at 80 kV.

Oblique section 3-D reconstruction procedure

Images were digitized on a Perkin-Elmer PDS 1010 M microdensitometer (Orbital Sciences Corp., Pomona, CA) at a step size corresponding to 1.25 nm with respect to the original object. The digitized images were preprocessed to remove density gradients across the image field. Images were processed using the crystallographic serial section reconstruction (CSSR) procedure as previously described (Taylor and Crowther, 1991). The magnitude of the gradient was determined using the 38.7 nm axial repeat, which has both actin- and myosin-based contributions. The direction of the gradient axis, which is the direction along which the section samples the 3-D object density at the same level along the z axis, was determined visually by marking off the positions of unit cells that had the same appearance in the micrograph. The absolute hand of the reconstruction was determined using the known hand of the actin target lattice.

Methods are available for calculating the section thickness and deconvoluting the reconstruction (Taylor and Crowther, 1991), thereby improving the axial resolution. Those methods require fairly high symmetry in the specimen. However, the mismatch between the fourfold symmetry of the myosin helix and the sixfold symmetry of the actin target helix results in a structure with low crystallographic symmetry. Thus, the methods used to determine section thickness in the case of rigor muscle, which has high symmetry, were not sufficient for this specimen. Therefore, we calculated the 3-D images without deconvoluting the effect of section thickness.

All CSSR calculations were done on a Silicon Graphics (Mountain View, CA) 4D35TG Personal Iris and 4D440GTX workstation. Surface images were computed with the EXPLORER software package.

Rotational averaging of thick filaments

Averaged thick filament profiles were obtained following procedures described by Schmitz et al. (1993). In this procedure, thick filaments are first windowed from the digitized image and their centers aligned using the SPIDER software package (Frank et al., 1981). The filaments were then examined for rotational symmetry of the outer wall region (radius 7–10 nm) using software provided by M. Stewart and F. A. Ashton. SPIDER was also used for sixfold symmetry filtering and superimposing images. For each filament, a power spectrum was generated showing the frequency components of the image at each radius, as well as the totals over all radii. Filaments that showed sixfold rotational symmetry were so filtered, and the filtered images were used to determine the angle necessary to rotate the gap of the outer wall subunits to the 12 o'clock position. The unfiltered images were then rotated to that angle and averaged using SPIDER procedures. All rotational filtering calculations were carried out on a VAXstation 4000 (Digital Equipment Corp., Woburn, MA).

RESULTS

Features of TAURAC-fixed muscle

The preservation of native thick filament features in TAURAC-fixed, relaxed IFM is best revealed in the "myac" layer, a 20–25 nm longitudinal section containing alternating myosin and actin filaments. In myac layers from relaxed muscle, the TAURAC procedure preserves a very regular 14.5 nm axial repeat of cross-bridges along each thick filament that only becomes obscured in the terminal 150–200 nm (Fig. 1). This 14.5 nm axial repeat is in very good lateral register across the entire myofibril. The 38.7 nm x-ray layer line in native, relaxed muscle contains contributions from three sources, 1) the helical arrangement of actin monomers on the thin filament, 2) the helical arrangement of myosin heads on the thick filament, and 3) cross-bridge labeling of the actin target zones (M. K. Reedy et al., 1992). Optical diffraction patterns from EMs of TAURAC-relaxed muscle reveal a strong 38.7 nm layer line suggesting excellent preservation of one or more of these features. The well preserved thick filament helix is the subject of our paper.

TAURAC fixation also enhances a 38.7 nm labeling of actin target zones by attached cross-bridges, presumably trapping weakly bound cross-bridge contacts that occur at low prevalence in native relaxed muscle. This enhancement is even more pronounced than with aldehyde fixation of relaxed IFM (Reedy et al., 1983), as shown elsewhere (Reedy, 1994) by x-ray diffraction monitoring of fixation, by EMs of actin layers, and by the absence of such labeling in cryofixed relaxed fibers. Attached cross-bridges in TAURAC-relaxed muscle typically appear in rows parallel to the Z-band with a distinct 38.7 nm axial repeat period (*arrows* in Fig. 1). The cross-bridges are smaller than those formed in rigor (Reedy and Reedy, 1985) or in strongly bound nucleotide states such as aqueous AMPPNP at room temperature (M. C. Reedy et al., 1987, 1988) and do not show the doublet grouping typical of rigor chevrons. This would suggest that only one myosin head is attached to each actin target. The basic 116 nm axial repeat of IFM contains 18 actin targets and 64 myosin heads so that complete labeling of actin targets by one myosin head would result in only 28% attachment.

Oblique transverse sections through relaxed TAURAC-fixed muscle display a superlattice pattern indicating a 3-D helical arrangement of features in the specimen (Figs. 2 and 3). The resemblance to similar sections of rigor makes it clear that some of the ordered mass corresponds to the cross-bridges attached every 38.7 nm to thin filaments as seen in longitudinal sections of relaxed muscle (*arrows* in Figs. 2 and 3). Density connecting thick and thin filaments appears straight rather than bent and slewed as in rigor muscle. However, there seem to be fewer cross-bridges per level than seen in oblique sections of rigor muscle (Taylor et al., 1993), and these cross-bridges appear less prominent, suggesting again that much of the myosin head mass is not attached to actin. The presence of this superlattice demonstrates that a 3-D image can be formed using oblique section reconstruction.

Oblique section image processing

We used the CSSR procedure for producing the 3-D images (Taylor and Crowther, 1991). In CSSR, unit cells in the 2-D image are averaged only along the direction perpendicular to the section gradient. This method of averaging ensures that cells are averaged only if their coordinate along the filament axis is the same. The result of this averaging is called a strip image because it is usually 1–2 unit cells wide and as long as the oblique section itself. The process of stacking successive sections from the strip image produces a 3-D reconstruction. CSSRs are obtained without use of space group

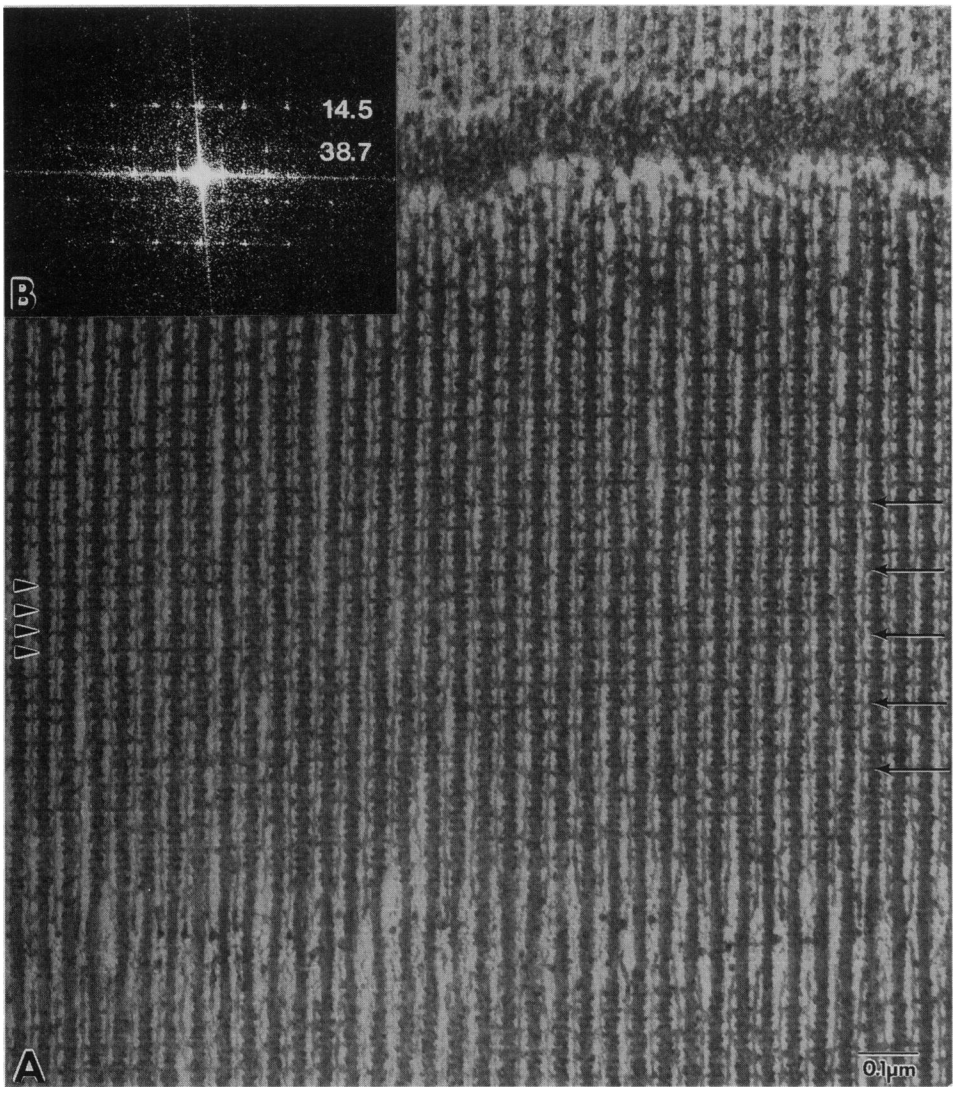

FIGURE 1 (*A*) EM and optical diffraction of TAURAC-fixed relaxed IFM of *Lethocerus*. The EM shows a myac single filament layer from a ~20 nm thick longitudinal section. TAURAC-fixed relaxed muscle reveals a very regular 14.5 nm axial repeat of cross-bridges that only becomes obscured in the terminal 150–200 nm at thick filament ends. Furthermore, a 38.7-nm repeat is present, produced by labeling of thin filaments by attached cross-bridges. These attached cross-bridges typically appear to emerge in rows with a distinctive spacing parallel to the Z-band marked by arrowheads on the left hand side. The vernier produced by the beating of 14.5- and 38.7-nm repeats produces a 116 nm long repeat marked by the arrows on the right hand side. (*B*) Optical diffraction demonstrates that the 14.5- and 38.7-nm periods dominate. There is very little, if any, intensity in the 19.3 nm layer line that is strong in rigor muscle.

symmetry, requiring only a knowledge of the unit cell dimensions and hand. In addition, the CSSR produces a 3-D image without averaging successive unit cells along the *c* axis period, thereby imaging unsymmetrized structures along the long 116 nm filament repeat. Although the reconstruction is not averaged along the *c* axis, the presence of repeating features in that direction implies an ordered 3-D lattice across the entire myofibril.

CSSR can produce a 3-D image from a single EM but requires that the section geometry satisfy certain restrictions on orientation with respect to the cell axes. Currently available procedures for processing hexagonal unit cells require that the section gradient is oriented in one of two ways. One allowed orientation has the section gradient running perpendicular to the *a* cell axis, whereas the other has the gradient oriented parallel to the *b* cell axis. Orientations that are less exact cannot be reconstructed with present methods, although adaptations could in principle be made to facilitate a broader application of this technique. As with the rigor IFM work done earlier (Taylor et al., 1993), we obtained two oblique transverse sections that satisfied the geometry requirement.

The first oblique section (Fig. 2) came from an image with a section gradient of 8° that was oriented perpendicular to the *a* cell axis. By virtue of the magnitude of this section gradient, we were able to reconstruct 360 nm of unit cell along the filament axis. An advantage of the CSSR method is that it can reconstruct areas of differing structure in the lattice as long as they have the same *a* and *b* unit cell dimensions. For example, the fibril shown in Fig. 2 contains both M-band and A-band features. Because the center of the thick filament backbone is sufficient to define the unit cell boundaries, a reconstruction showing both M-band and A-band is easily obtained. All that is necessary is a large enough stretch of A-band to determine the sign and the magnitude of the section gradient.

We used a modified averaging procedure to obtain a 3-D image of this first myofibril. The superlattice is very regular across large regions of the fibril, but the cylindrical nature of the fibril, which was too large to photograph on the film at this magnification, plus some irregularities in the superlattice caused by the sectioning process made it difficult to average the same number of unit cells in each level. We resorted, therefore, to averaging regions of different numbers

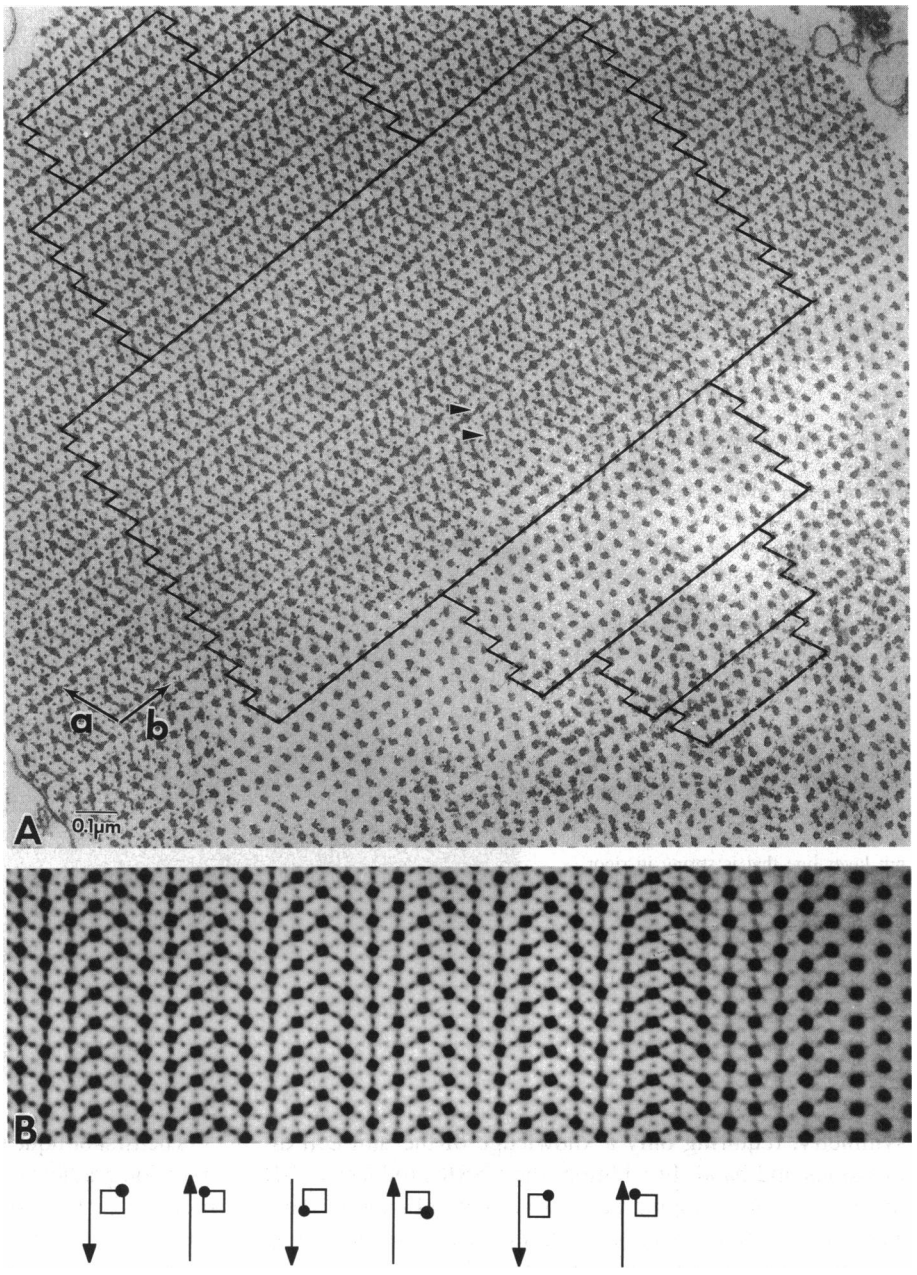

FIGURE 2 (*A*) EM of an oblique cross section of TAURAC-fixed relaxed IFM. This cross section cuts through the M-band and the A-band of the muscle fiber. The section is about 15 nm thick. Structures in the M-band seem to be very disordered, although an oval profile of the myosin filaments is present. In the A-band, cross-bridge densities are visible at some levels (*arrowheads*), suggesting that even in this TAURAC-relaxed state there are some cross-bridges attached to the actin filaments. We chose to average regions of different numbers of unit cells at different levels along the section gradient. The dimensions of these different regions are mapped on the EM image. Arrows mark the *a* and *b* cell axes. (*B*) Resulting strip image after crystallographic serial section reconstruction. Arrows and squares at the bottom mark successive left-handed, 180° rotations of actin targets (*arrows*) and right-handed 90° rotations of tetragonal myosin crowns (*squares*), respectively, progressing from left to right across the filtered strip image. Note that a full 360° anticlockwise rotation of crowns encompasses 2 × 360° clockwise rotation of actin targets.

of unit cells at each level along the section gradient (Fig. 2). These regions were always contiguous, thereby ensuring that they could be stacked successively to produce a single reconstruction. They only differed in the width of the area averaged. This procedure, which facilitates the process of maintaining the superlattice regularity, also means that the signal-to-noise ratio is different for different regions of the reconstructed image.

The second image selected had a section gradient of 6° oriented parallel to the *b* cell axis and was reconstructed by averaging the image into two strip images that were interleaved to improve the sampling along the filament axis (Fig. 3). This image, which reconstructed a length of 207 nm along the filament axis, included only the A-band. The number of cells averaged laterally for this image was the same along the entire volume reconstructed.

One of the intermediate steps in the CSSR procedure is the production of an averaged strip image (Figs. 2 *B* and 3 *B*). This strip image exhibits all of the 3-D information contained within the reconstruction but in the form of a 2-D display. The strip images calculated for the two oblique sections reveal two helical systems of opposite sense along each thick filament. One of these is the myosin filament helix (Fig. 4 *A*). The other is the actin target helix (Fig. 4 *B*).

The superlattice pattern that dominates the original image as well as the averaged strip image arises primarily from the interfilament density of cross-bridges. As the gradient of the oblique section progresses through successive unit cells along the filament axis, cross-bridge density rotates reflecting the binding of myosin heads along the helical array of actin target zones around the thick filament (Figs. 2, 3, and 4 *C*). Because the actin target helix is of known hand (M. K.

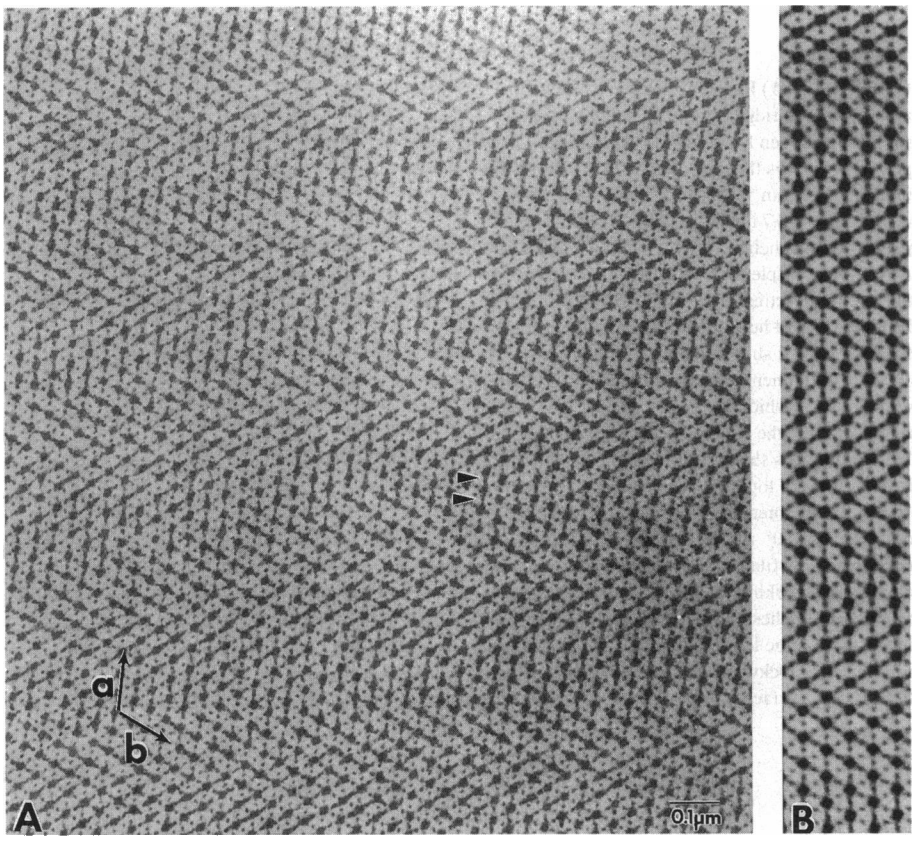

FIGURE 3 (*A*) EM of an ~15 nm thick oblique cross section through an A-band of TAURAC-fixed relaxed IFM. As in Fig. 2, cross-bridge densities are visible at different levels (*arrowheads*), confirming that in TAURAC-relaxed muscle there is a regular pattern of cross-bridges attached to the actin filaments. Arrows mark the *a* and *b* cell axes. (*B*) Resulting strip image after crystallographic serial section reconstruction.

Reedy, 1968), this rotation can be used to assign an absolute hand to the reconstruction.

A second helix is observed on the myosin filaments. Each myosin filament in the averaged strip image reveals a square profile indicative of a fourfold arrangement of myosin projections from the filament backbone (Fig. 2 *B*, 3 *B*, and 4). This squarish appearance agrees with the symmetrical arrangement of four pairs of myosin heads in each 14.5-nm layer (Wray, 1979a; Morris et al., 1991). Because these are largely not attached to actin, they thereby conform to a fourfold screw symmetry on the thick filament surface rather than the sixfold screw symmetry of the actin target lattice. In the progression along the gradient of the strip image, the squarish profiles rotate in accord with the helical surface lattice. Compared with the actin target lattice, the sense of rotation is opposite, the helix repeat is the same at 38.7 nm, but the pitch is twice as long because the helix is four-stranded instead of two-stranded (Fig. 4). This is exactly as proposed by Wray (1979a) and found in isolated thick filaments by Morris et al. (1991) and M. K. Reedy et al. (1993) for the thick filament helix.

The CSSR from the oblique section comprising M-region and A-band (Fig. 2) reveals another feature: in the M-region, there is little evidence of M-bridges that presumably are present to hold the structure together. In addition, the averaged thick filament shaft has a round profile rather than the oval profile visualized in the original image. The loss of oval profiles in the M-region of the averaged image is expected given the disordered arrangement seen here and observed originally by Freundlich and Squire (1983).

Rotational averaging of thick filaments

The subfilament structure in the thick filament backbone has low intrinsic contrast so that previous work to establish the rotational symmetry of thick filaments in IFM used relatively thick sections as well as a different protocol for preserving the filament structure (Beinbrech et al., 1988, 1990, 1992; Schmitz et al., 1993, 1994). We wanted to determine if (1) the TAURAC protocol also preserved this feature and (2) whether any backbone structure could be observed in a thin section. The sections used in the present work are 6- to 10-fold thinner than those used previously so that demonstration of subfilament structure and its relative orientation among the different thick filaments is potentially more difficult. In addition, any surface distortions caused by sectioning are potentially more significant in a thin section than they would be for a thick section. For this calculation, we selected the oblique section image with the lowest gradient (Fig. 3) to minimize misorientation effects. These would in any case be less severe in a thin section than in a thick section. 200 filaments were windowed, and their rotational power spectra were calculated. Out of this population of images, 140 (70%) showed significant sixfold symmetry for the region outer wall (Fig. 5 *A*). The 12-fold power, however, was usually insignificant. Those images that revealed sixfold

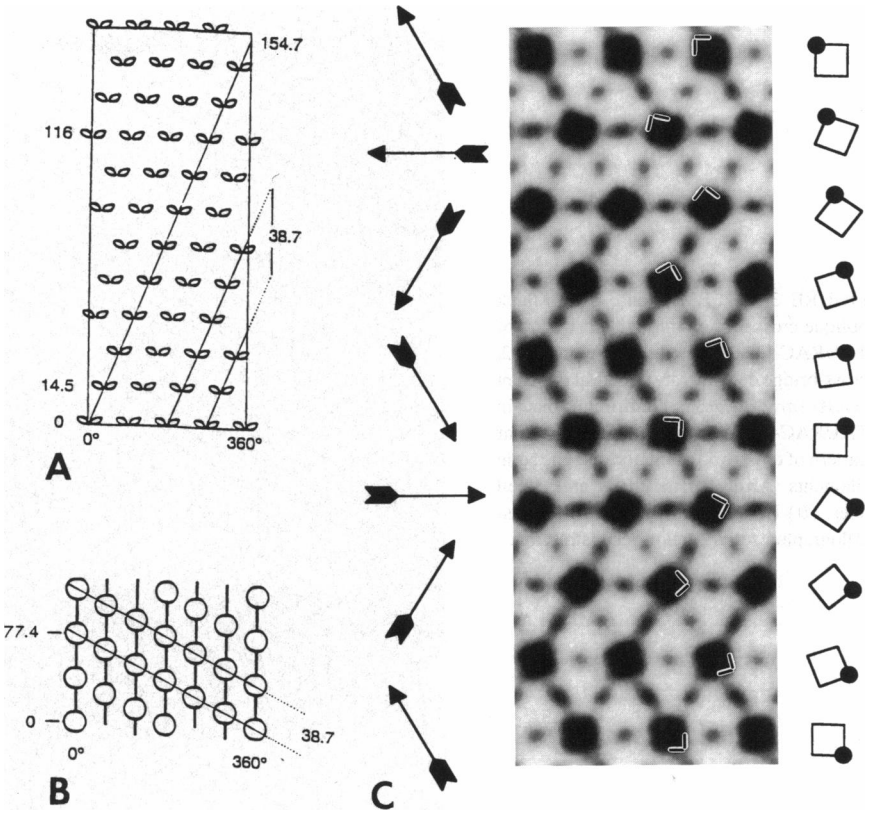

FIGURE 4 (*A*) Radial projection of the helical array of cross-bridge origins on *Lethocerus* myosin filaments seen from outside the filament. The projection shows the four-stranded filament with the 8 × 14.5 nm repeat. The lines indicate the right-handed 38.7 nm helical rise. (*B*) Radial projection of the helical array of actin targets in *Lethocerus* muscle seen from outside the cage of the 6 orbital actins. The lines indicate the left-handed 38.7 nm helical rise. (*C*) Enlargement of the interpolated strip image of Fig. 2 (*B*). Averaged thick filaments have a squarish profile, the orientation of which is marked by the "V" in the figure and by the marked squares to the right. Square fiducials show the anticlockwise rotation from bottom to top of a right-handed helix. The 10 rows of filaments contained in the figure undergo a net 180° rotation. Weak densities connecting myosin filaments with actin filaments are also visible marking the actin target lattice. The orientation of these cross-bridges is marked by the arrows on the left. Note that the target lattice rotates 360° clockwise over the same distance as the myosin surface helix rotates anticlockwise 180°.

symmetry in the outer wall were then rotationally aligned by determining the angle that oriented the sixfold densities. The distribution of azimuths determined from this alignment was essentially random across any particular row of filaments (where the position along the filament axis is constant) and totally random across the entire fibril (Fig. 5 *B*), as found previously (Schmitz et al., 1994). To create an average image, 38 filaments that revealed the highest sixfold power were rotated and superimposed. After averaging, there was, as expected, a significant improvement in the sixfold power (Fig. 5 *C*). The averaged image (Fig. 5 *D*) shows six strong density spots in the outer wall, which we interpret as the myosin subfilaments, and strong density spots in the inner wall, which we believe correspond to some of the paramyosin filaments, apparently five in number, thought to occupy the inner wall (Schmitz et al., 1994). In keeping with the very low 12-fold power in the thick filament profiles, there was no subdivision of the six subfilaments into a pair of densities. The remaining 102 images, averaged as a second set, had similar features but with less contrast (not shown). Given the limitations because of the thickness of these sections, we consider these results, i.e., random rotational orientation and six subfilaments, to be substantially in agreement with previous results (Beinbrech et al., 1988, 1990, 1992; Schmitz et al., 1993, 1994).

3-D reconstruction

The two major features of the 3-D reconstruction, myosin helix and cross-bridges, become much more obvious in surface images of myac layers (Fig. 6). The averaged myosin filament displays the right-handed, four-stranded helical tracks of the cross-bridge origins on the filament surface that arise from the regular rotation of the square profiles (Fig. 6 *A*). Because CSSR averages all myosin filaments of one row in the original oblique section together, the orientation of myosin heads of all filaments in a specific row is about the same; otherwise, an average would show round profiles. In other words, the cross-bridges on the surfaces of myosin filaments in the same row, corresponding to one axial level, have to be in register to get an averaged square profile. Because the image is averaged over the entire myofibril, these two features, square profiles and their continuous rotation, could only be observed if the cross-bridges on the surface of the myosin filaments are in helical register across the entire 2-D array of filaments in the fibril.

The typical appearance of cross-bridges in TAURAC-relaxed IFM is very different from that of rigor muscle (Taylor et al., 1989a, 1993), but the resolution along the filament axis is much lower in the present work. The transform of TAURAC-fixed relaxed muscle consists of mainly the equator, 38.7 nm-, and 14.5 nm layer planes. Because the 15 nm section thickness has reduced the contrast substantially on the 14.5 nm layer plane, we judge the axial resolution to be ~18 nm. The distinct double-chevron pattern as well as the well defined triangular shape of the lead bridges of rigor muscle are not observed (Fig. 6 *B*), suggesting that the rigor bridge shape is not a feature of relaxed muscle. Even at the low density contour threshold used to display the cross-bridges, they appear much less substantial than those seen in

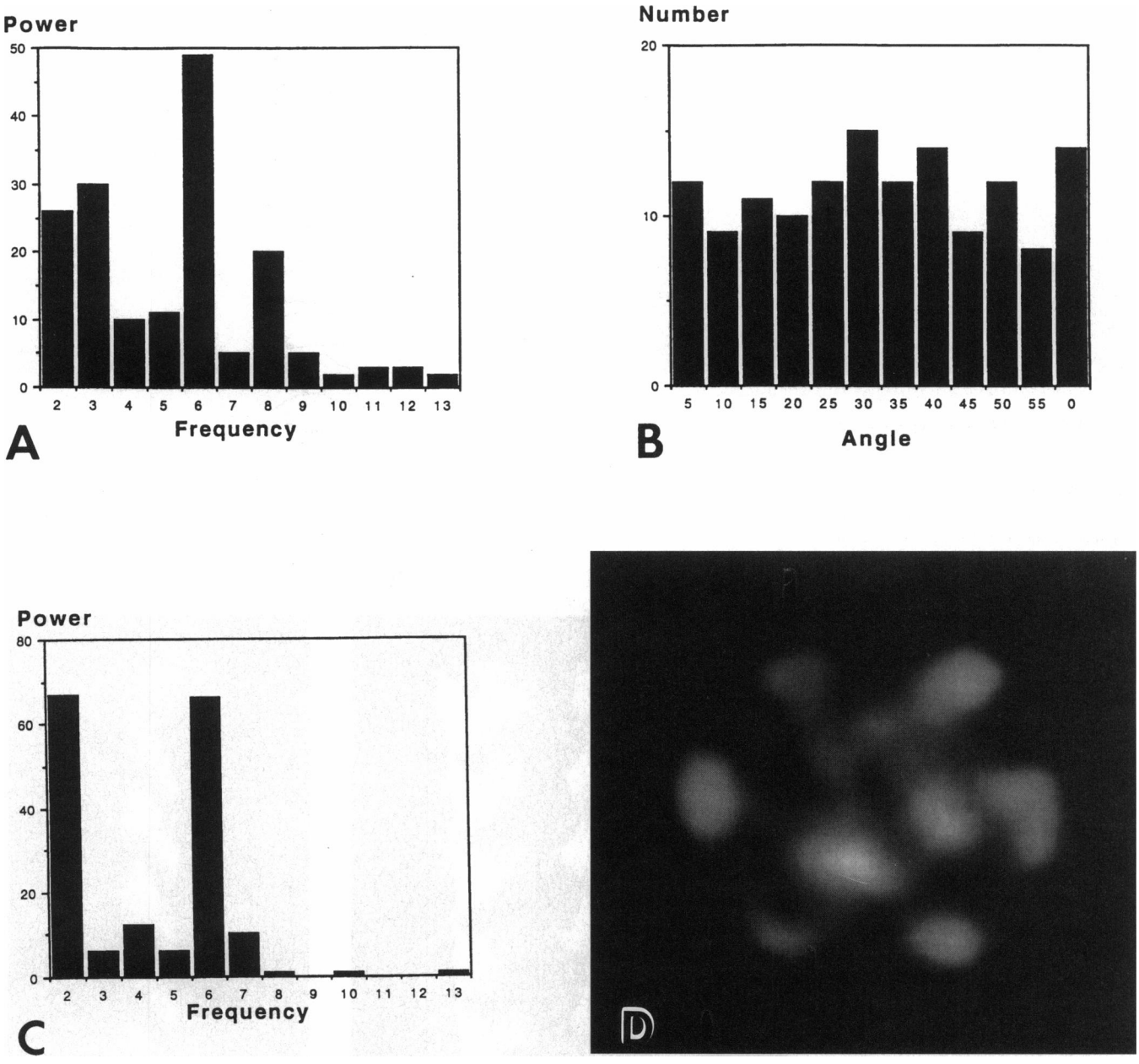

FIGURE 5 (*A*) Rotational power spectrum as a function of frequency for the outer wall (radius 14–20 nm) of a typical TAURAC-fixed *Lethocerus* myosin filament. (*B*) Angular distribution of myosin filament profiles. Shown here is a histogram of the angles that were necessary to orient the sixfold densities in the outer wall to the 12 o'clock position. A total of 140 filaments are included in this distribution. (*C*) Rotational power spectrum as a function of frequency for the outer wall (radius 14–20 nm) for the average image of the 38 best myosin filaments shown in *D*. (*D*) Average image after superimposing 38 myosin filaments. Six density spots can be seen in the region of the outer wall, which we interpret as the myosin subfilaments. The density spots in the inner wall of the image correspond to the paramyosin filaments.

rigor IFM. A fairly distinct left-handed 38.7-nm helix is visible on the thick filament, but this feature arises from the limited cross-bridge formation, which conforms to the symmetry of the actin target helix. At a higher contour threshold, the fourfold symmetry near the thick filament surface is uninterrupted even with limited cross-bridge attachment (Fig. 6 *C*) so that much of the cross-bridge mass remains docked with the thick filament origin. The cross-bridges of one level all have the same relative height and come out of the filament surface at the same average axial angle of ~90°. These observations suggest that the cross-bridges comprise only single myosin heads attached to the actin filaments.

The 3-D reconstructions reveal only weak periodicity at 14.5 nm axial spacing, which would arise from the spacing between successive levels of myosin heads. The 14.5 nm periodicity is weak because the ~15 nm section thickness is close to that of the 14.5 nm axial period. In oblique section reconstruction, features at axial spacings that are close to the thickness of the section have weak or no contrast. This phenomenon occurs because the entire period is contained within

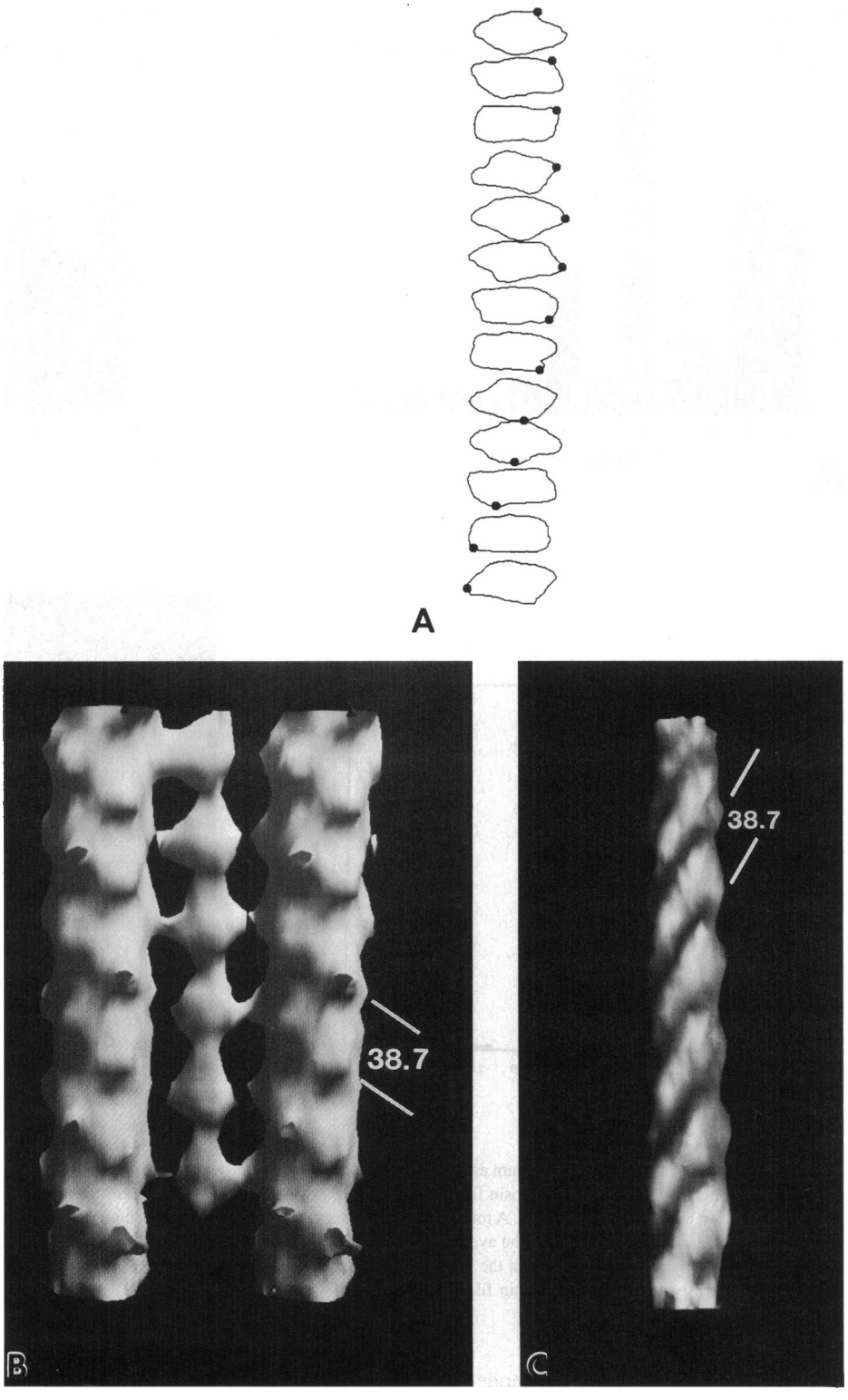

FIGURE 6 (*A*) Contour representation of the reconstruction showing the right-handed, helical arrangement of the squarish profiles. (*B*) 3-D surface reconstruction of parts of two myosin filaments and an intermediate actin filament. On the surface of the myosin filaments we see the left-handed helix of the actin targets as well as densities representing the origins of the cross-bridges. These origins of the cross-bridges are in register. The small cross-bridges that attach to the actin filament have low density even at this contour level and lack the triangular shape typical of rigor. This suggests that they comprise no more than one head. (*C*) 3-D surface reconstruction of a myosin filament, showing the right-handed, four-stranded 38.7 nm helical tracks of the cross-bridge origins, which arise from the regular arrangement of the square profiles.

the section so that the peaks and valleys of density that make up the period cannot be sampled separately. Deconvolution can improve the resolution when the section thickness is accurately known. We did not attempt deconvolution because an accurate measure of the section thickness was not available. Moreover, the contrast of the 14.5 nm axial period would be weak even with deconvolution, so there would have been very little benefit in attempting this.

The successively rotated square profiles seen in strip images (Figs. 2–4) and derived from the reconstruction (Fig. 6) do not correspond to individual crowns spaced 14.5 nm axially. The strip image profile rotates by a variable amount depending on the section gradient and presents the thick filament somewhat as if it were a smoothly twisted rod of square profile at every level. More satisfying detail resolving crowns from intercrown shaft of myosin filaments is

expected from procedures now being developed to combine oblique transverse sections with oblique longitudinal sections (Winkler and Taylor, 1994).

DISCUSSION

The structure of *Lethocerus* thick filaments in the relaxed state is distinct from, but related to, those seen in other invertebrate and vertebrate thick filaments. Like several other arthropod thick filaments (Crowther et al., 1985; Kensler et al., 1985), those from *Lethocerus* have four pairs of myosin heads arranged axially with a spacing of 14.5 nm (Wray, 1979b; M. K. Reedy et al., 1981, 1993; Morris et al., 1991). However, the myosin heads in *Lethocerus* thick filaments are arranged in a manner to give distinct perpendicular shelves of density every 14.5 nm, thereby giving rise to a very strong meridional reflection with that spacing in x-ray diagrams of relaxed muscle and in diffraction patterns from EMs of thin sections (M. C. Reedy et al., 1987; M. K. Reedy et al., 1993) as well as isolated thick filaments (Morris et al., 1991). In addition, the four-stranded helices in *Lethocerus* are separated axially by 38.7 nm, giving an integral repeat every 8 $\times$ 14.5 nm, whereas those of other arthropods are separated by 43.5 nm, giving an integral repeat every 3 $\times$ 14.5 nm.

In this study, we used a relatively new fixation procedure, the TAURAC method (M. K. Reedy et al., 1991), which preserves a relaxed state of the flight muscles, but traps some myosin heads attached to actin. The longitudinal sections of this muscle produce a diffraction pattern with both 38.7- and 14.5 nm layer lines. Two sources contribute to diffraction on the 38.7 nm layer line. Some of this intensity comes from the 38.7 nm-based helices of actin filaments decorated by attached cross-bridges, and the increased decoration after TAURAC fixation is associated with increased intensity of this layer line. Additional contribution comes from the 38.7 nm layer line that arises from the helical arrangement of myosin heads on the thick filament surface (M. K. Reedy et al., 1993). The 14.5 nm layer line is related to the origins of the cross-bridges on the myosin filament surface (Wray, 1979b). This 14.5-nm repeat of the cross-bridges, which is characteristic for relaxed muscles, is well preserved.

The striking point about the reconstruction is that, on average, the cross-bridges of all the filaments in the A-band lattice are in helical register. Only averaging filaments with the same orientation of the cross-bridges maintained across the whole of each row would lead to an averaged myosin filament with this squarish profile. This finding of highly ordered cross-bridges in the filament lattice (A-band) is somewhat surprising, considering previous observations of disorder in the arrangement of myosin filament backbones.

The thick filaments of *Lethocerus* in the M-band region show oval profiles in cross section (Freundlich and Squire, 1983). Freundlich and Squire studied the orientations of these oval profiles and showed that they were distributed in a random-biased manner over three different orientations 60° apart. They also concluded that this distribution would extend into the A-band. Because myosin molecules are spaced 90° apart at each 14.5 nm axial level, the random-biased distribution of myosin filaments based on 60° rotations would result in an irregular arrangement of myosin heads in the A-band with misalignments of the order of 30°. The observation made here that oval profiles of individual myosin filaments in the unprocessed image of the M-band averaged out to circular profiles in the reconstruction is consistent with the observations of Freundlich and Squire (1983).

However, later studies (Beinbrech et al., 1988, 1990, 1992; Schmitz et al., 1993, 1994) investigated the rotational symmetry and orientation of myosin filament backbones in the A-band of flight muscle from several insect species. These groups observed sixfold rotational symmetry of the filament backbones in every insect examined and a totally random distribution of azimuthal rotations of the backbones for *Musca* (Beinbrech et al., 1990), *Apis*, *Phormia*, and *Lethocerus* (Schmitz et al., 1994). In the present work, we also observe this disorder in TAURAC-fixed *Lethocerus* IFM. This totally random distribution is a much greater degree of disorder than could be predicted based on the M-band structure. We would conclude from this that the M-band is not an accurate predictor of cross-bridge orientation in the A-band. This suggests that the oval thick filament profiles in the M-band are caused by an accessory protein that is more regularly oriented rotationally than the backbone itself.

The two types of thick filament disorder detected in IFM, M-band and backbone rotation, might be expected to randomize the cross-bridge origins at any particular axial level and predict that the average thick filament profile should be circular. Such a profile is not observed but, instead, the azimuthal rotations of the averaged cross-bridge origins are in a remarkable degree of helical register across the A-band. It is nevertheless paradoxical at first sight that IFM can reveal such a regular attachment of cross-bridges starting from such predicted disorder in cross-bridge origins.

How can we reconcile the conflicting observations of a rotationally ordered population of cross-bridges originating from a rotationally disordered arrangement of filament backbones (Fig. 7), when both myosin head symmetry and backbone subfilament symmetry should each be derived in a uniform way from the same underlying regular packing of myosin molecules? These observations can be reconciled if the azimuthal orientation of myosin filaments is optimized for interaction of myosin heads with the actin target lattice rather than formation of M-bridges. We assume that the first, second, third, etc. square crowns starting at the bare zone each have a well defined, fixed relationship to the myosins packed into the sixfold subfilament arrangement in the backbone. The disorder may then arise in two ways. First, the fourfold myosin crowns can rotate to four different positions 90° apart within the sixfold actin targets yet keep identical relationships between cross-bridge origins and attachments, while producing two orientations of sixfold backbones that

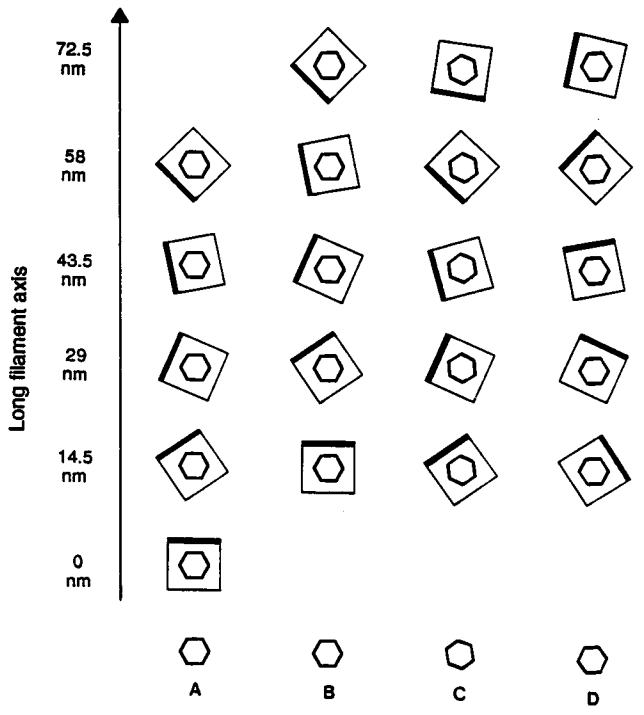

FIGURE 7 Schematic model of the orientation of myosin filaments (*A–D*) in IFM. Part of each filament is represented as a series of sections, 14.5 nm apart. Hexagons represent the filament backbone, whereas the squares represent the crowns of myosin heads (see Fig. 4), which are 14.5 nm apart. As described, the squarish arrangement of cross-bridges rotates in a right-handed way, 33.75° every 14.5 nm. Considering two adjacent myosin filaments, *A* and *B*, staggered by 14.5 nm, with the same orientation of the backbones, the staggering would introduce a 33.75° disorder in the azimuthal arrangement of myosin heads between these two filaments. A reorientation of the thick filaments (*C*) to align the cross-bridges with actin targets would lead to a 33.75° disorder in the backbones, whereas the squares would come into rotational register with *A*, as observed. A rotation by 90° of the fourfold myosin filaments (*D*) will introduce an additional ±30° rotation of the backbones but leave myosin heads situated just as in *A* or *C* with respect to the actin target lattice. If up to 7 displacements of 14.5 nm can occur in combination with the 30° randomization, the apparently random rotation arrangement of backbones can be generated and still preserve a regular arrangement of the origins of myosin heads. The resulting orientations of the backbones after alignment of the filaments are shown at the bottom part of the diagram.

differ by ±90° (=±30° for a hexagon). Further randomization could arise in the following manner. Suppose the ideal sarcomere begins with all thick filaments in perfect axial register and rotational alignment. Real A-bands, even in unstretched, relaxed muscle, depart from this ideal state in at least one way that is obvious in longitudinal sections: the ends and M-band thickenings of neighboring thick filaments are often a little out of axial register (e.g., EMs in M. K. Reedy 1967; Haselgrove and Reedy, 1984), always by small multiples of 14.5 nm so this period stays in register between filaments, even when the offset accumulates to 5–7 × 14.5 nm or more across the myofibril. How can this occur without disturbing the 38.7- and 116-nm repeats of attached cross-bridges, and especially without disturbing the helical register demonstrated here? A simple explanation that seems inescapable is that the staggered filaments must undergo screw displacements rather than strictly axial ones, so that each axial offset of 14.5 nm is accompanied by a ±33.75° rotation that exactly follows the thick filament surface lattice. Then, regardless of net axial stagger between thick filaments, the overlap zone would exhibit exact helical register, and the 38.7- and 116-nm repeats would continue to indicate unchanging relative positions between cross-bridge origins and actin targets. (The Note added in proof of Haselgrove and Reedy (1984) discussed this clearly enough except for the now mystifying mention of 56.25° rotations and 29-nm displacements.) To say the evidence points to this leaves for later the problem of explaining what dynamic in their shared interactions with the actin target lattice might constrain thick filaments to lattice-preserving screw displacements rather than simple but lattice-breaking axial displacements. But now we have an explanation for apparently random rotational orientation of the sixfold backbones in thick filaments. If, in the primitive "ideal" state, a single transverse level starts with an identical relative alignment of square crowns to hexagonal backbones in all thick filaments, the screw displacements just proposed would rotate adjacent backbones by $N \times 33.75°$, N representing the number of 14.5-nm displacements, causing non-sixfold rotations of backbones that would obscure their "original" alignment and make them appear randomly oriented while preserving perfect helical register among all thick filaments. If up to seven displacements of 14.5 nm can occur in combination with the 90° randomization allowed by the fourfold rotational symmetry of the thick filament, then fourteen different rotational presentations of sixfold backbones could be generated. If all are equally probable, the result would be indistinguishable from randomized rotations, yet perfectly compatible with a regular arrangement of myosin head origins.

What known features of IFM could conceivably produce this ordered arrangement of cross-bridges from rotationally disordered myosin filaments? In striated muscles, the Z-band serves to link the polar array of actin filaments in half of one sarcomere to the array of actin filaments with opposite polarity in the adjacent sarcomere along the myofibril. Z-band attachments probably determine the three-dimensional lattice of actin filaments and, thus, of actin target zones in the sarcomere. Thus, the Z-band may control much of the geometry of interaction of myosin cross-bridges with actin in active or rigor muscle.

In contrast to the disorder detected in the IFM thick filament lattice as filament misregistration or randomized backbone rotations, the thin filaments in *Lethocerus* muscle keep a very regular arrangement with at most a 180° azimuthal disorder (Holmes et al., 1980; M. K. Reedy, 1968). This 180° azimuthal disorder will have little effect on thick filament ordering because the pseudo-twofold symmetry of actin filaments fits imperceptibly (at any resolution worse than ~3 nm) into the twofold lattice positions between adjacent thick filaments. The actin target zones form a regular set of left-handed doubled helical tracks around a myosin filament. We

have seen that in TAURAC-relaxed muscle a definite fraction of cross-bridges appear to be attached to these actin targets, forming a regular lattice suggested by longitudinal sections (Fig. 1), reconstructed in 3-D from oblique transverse sections (Fig. 6) and fully congruent with the lattice labeled in rigor by cross-bridges of a different shape and number. It is conceivable that the actin target lattice is not just available to, but governs to some degree, the orientation of myosin filaments in the IFM lattice, based on some dynamic like the "annealing to maximize the number of cross-bridge interactions" suggested by Haselgrove and Reedy (1984). However, taken alone, that dynamic is insufficient to explain lateral and helical register, because it can only drive thick filaments to the nearest good fit with the actin target zone helix, without regard for the exact level of the 14.5 nm myosin repeat. This optimum fit must incorporate vernier variations between the eight levels of myosin crowns and the nine levels of actin targets per 116 nm. What is to prevent two thick filaments sharing a thin filament between them from asymmetrically choosing two different options from among these nine as they contact the two sides of one target zone? The symmetry we observe demands lateral register of 14.5 nm myosin crowns, combined with helical register, to achieve the exact alignment that brings 116-nm variations in presentation of 38.7- and 14.5-nm repeats into lateral register.

The helix-matching hypothesis of stretch activation is similarly insensitive to 14.5- and 116-nm aspects of myosin crown level, requiring only that the myosin surface helix match the actin target helix to the best fit every 38.7 nm or every 90° of thick filament positioning (Wray, 1979b; Abbott and Cage, 1984). This hypothesis has come under recent scrutiny in terms of alternative thin filament lattices thought to exist in IFM (Squire, 1992), but nothing explanatory for our problem has emerged. What needs to be explained is how an axially unspecified but helically optimum fitting of the myosin surface helix to the actin target helix should anneal to the same exact axial and azimuthal vernier as all other thick filaments.

Several possible effects might be pertinent. (1) Disregarding the randomized 60° rotations of M-band profiles, can M-band bridges alone suffice to stabilize thick filament rotational alignment in *Lethocerus* IFM? This seems unlikely; their 60° symmetry appears poorly fitted to recognize variations in thick filament rotation implied by the indications for lattice-preserving screw displacements. Their obvious role is that M-bridges must passively accommodate rotational and azimuthal readjustments in the overlap zone, even detaching and reattaching on other M-bridging sites when necessary. (2) The alignment in relaxed muscle might depend on a "memory" effect annealed in during previous strongly binding cross-bridge attachments. Beinbrech et al. (1990) observed that sixfold filament backbones in rigorized *Musca* flight muscles showed some preferential alignment with respect to the myofilament lattice, unlike the randomly oriented backbones in relaxed specimens. However, the fibers used in our study were never rigorized, so that persistence of rigor effects cannot be invoked here. Indeed, it seems more likely that any persistence effect runs in the other direction, i.e., that the helical registration in relaxed muscle precedes and gives rise to the helical registration manifested in rigor by lateral register of the 116 nm repeat. (3) Bullard et al. (1988) have suggested that troponin-H (TnH), an unusual troponin species found in insects, may provide a mechanical link between the myosin helix and the target helix. TnH is thought to have an extended domain that might function as a mechanical linker between the thin filament regulatory complex and the head portion of myosin to sense stretch. Because TnH is periodic and very close to actin target zones on thin filaments by immunoEM (M. C. Reedy et al., 1994), it could also support registration between myosin and actin target helices. (4) A cooperative interaction might be transmitted between opposed cross-bridges or other linkages attached to the thin filament on opposite sides of the same target zone. However, even if opposing myosin heads could sense and mimic finely graded variations in binding geometry from opposite sides of a single target zone, the weakness and flexibility of myosin-actin binding in relaxed muscle would not be expected to enforce detailed azimuthal mimicry from one myosin backbone to its neighbor. (5) However, a two-part mechanism of which this was one part might operate. A tendency to maximize weakly binding relaxed myosin interactions to actin targets, in the way argued for rigor interactions by Haselgrove and Reedy (1984), would match myosin and target helices in an axially neutral fashion. This could be complemented by an independent tendency for neighboring thick filaments to bring their 14.5 nm repeats into axial register, by a myosin head-to-head or crown-to-crown interaction mediated through, around, or even bypassing the shared thin filament. Even a very weak association of this nature would be amplified by the $\sim 80 \times 14.5$ nm repeats in each half-sarcomere. This is, in fact, less speculative than the Haselgrove-Reedy "annealing," because in *Lethocerus* myofilament suspensions viewed in the EM by negative staining it is common to find parallel "rafts" of a few thick filaments bundled together with their 14.5 nm cross-bridge periods in excellent lateral register, sometimes with but often without a shared thin filament visible between them (M. K. Reedy, unpublished observations). The 14.5 nm repeat of M-bridges in *Lethocerus* might also suggest a role for these in axial matching of 14.5 nm myosin crown repeats, but M-bridges rarely survive on the half-filaments commonly found in negative stain preparations, nor could this operate in bee or fly IFM, where nonperiodic M-bands of very different structure are found. Obviously, an attractive test whether thick filament interactions alone can maintain register of periodic or even helical features between thick filaments may be possible using waterbug and bee IFM from which thin filaments have been selectively removed by gelsolin (Granzier and Wang, 1993).

Whatever its structural basis, it seems likely that preordering of cross-bridges in the relaxed state could enhance the

effectiveness of the whole sarcomere unit when activated to produce length-sensitive, stretch-activated oscillatory work.

The authors thank David Finley, Yun Zhang, and Melody Rice for technical assistance.

This research was supported by National Institutes of Health grants GM-30598 and AR-14317. The PDS 1010 M densitometer was purchased with funds from National Science Foundation grant PCM-8400167. The Silicon Graphics 4D440GTX work station was purchased through a grant from the Rippel Foundation to the Duke Molecular Biophysics Program. The VAX-station 4000 was purchased with funds from the North Carolina Biotechnology Center and the National Science Foundation.

REFERENCES

Abbott, R. H., and P. E. Cage. 1984. A possible mechanism of length activation in insect fibrillar muscle. *J. Muscle Res. Cell Motil.* 5: 387–397.

Auber, J. 1967. [Remarks on the structure of fibrils of the muscles of the insect wing, at the level of the M streak] (Fr). *C. R. Acad. Sci. (Paris).* 264:2916–2918.

Beinbrech, G., F. T. Ashton, and F. A. Pepe. 1988. The invertebrate myosin filament: subfilament arrangement in the wall of tubular filaments of insect flight muscles. *J. Mol. Biol.* 201:557–565.

Beinbrech, G., F. T. Ashton, and F. A. Pepe. 1990. Orientation of the backbone structure of myosin filaments in relaxed and rigor muscles of the housefly: evidence for non-equivalent crossbridge positions at the surface of thick filaments. *Tissue & Cell.* 22:803–810.

Beinbrech, G., F. T. Ashton, and F. A. Pepe. 1992. The invertebrate myosin filament: subfilament arrangement of the solid filaments of insect flight muscles. *Biophys. J.* 61:1495–1512.

Bullard, B., K. Leonard, A. Larkins, G. Butcher, C. Karlik, and E. Fyrberg. 1988. Troponin of asynchronous flight muscle. *J. Mol. Biol.* 204: 621–637.

Crowther, R. A., R. Padron, and R. Craig. 1985. Arrangement of the heads of myosin in relaxed thick filaments from tarantula muscle. *J. Mol. Biol.* 184:429–439.

Frank, J., B. Shimkin, and H. Douse. 1981. SPIDER—A modular software system for electron image processing. *Ultramicroscopy.* 6:343–358.

Freundlich, A., and J. M. Squire. 1983. Three-dimensional structure of the insect (*Lethocerus*) flight muscle M-band. *J. Mol. Biol.* 169: 439–453.

Granzier, H. L. M., and K. Wang. 1993. Interplay between passive tension and strong and weak binding crossbridges in insect indirect flight muscle. A functional dissection by gelsolin-mediated thin filament removal. *J. Gen. Physiol.* 101:235–270.

Haselgrove, J. C., and M. K. Reedy. 1978. Modeling rigor crossbridge patterns in muscle. Initial studies of the rigor lattice of insect flight muscle. *Biophys. J.* 24:713–728.

Haselgrove, J. C., and M. K. Reedy. 1984. Geometrical constraints affecting crossbridge formation in insect flight muscle. *J. Muscle Res. Cell Motil.* 5:3–24.

Holmes, K. C., D. Popp, W. Gebhard, and W. Kabsch. 1990. Atomic model of the actin filament. *Nature.* 347:44–49.

Holmes, K. C., R. T. Tregear, and J. Barrington-Leigh. 1980. Interpretation of the low angle x-ray diffraction from insect muscle in rigor. *Proc. R. Soc. Lond. B Biol. Sci.* 207:13–33.

Huxley, A. F. 1957. Muscle structure and theories of contraction. *Prog. Biophys. Biophys. Chem.* 7:255–318.

Kensler, R. W., R. J. C. Levine, and M. Stewart. 1985. Electron microscopic and optical diffraction analysis of the structure of scorpion muscle thick filaments. *J. Cell Biol.* 101:395–401.

Miller, A., and R. T. Tregear. 1972. The structure of insect fibrillar flight muscle in the presence and absence of ATP. *J. Mol. Biol.* 70: 85–104.

Morris, E. P., J. M. Squire, and G. W. Fuller. 1991. The 4-stranded helical arrangement of myosin heads on insect (*Lethocerus*) flight muscle thick filaments. *J. Struct. Biol.* 107:237–249.

Offer, G., and A. Elliott. 1978. Can a myosin molecule bind to two actin filaments? *Nature.* 271:325–329.

Rayment, I., W. R. Rypniewski, K. Schmidt-Baese, R. Smith, D. R. Tomchick, M. M. Benning, D. A. Winkelmann, G. Wesenberg, and H. M. Holden. 1993. Three-dimensional structure of myosin subfragment-1: a molecular motor. *Science.* 261:50–58.

Reedy, M. C., M. K. Reedy, and R. S. Goody. 1983. Co-ordinated electron microscopy and x-ray studies of glycerinated insect flight muscle. II. Electron microscopy and image reconstruction of muscle fibers fixed in rigor, in ATP and in AMPPNP. *J. Muscle Res. Cell Motil.* 4:55–81.

Reedy, M. C., M. K. Reedy, and R. S. Goody. 1987. The structure of insect flight muscle in the presence of AMPPNP. *J. Muscle Res. Cell Motil.* 8:473–503.

Reedy, M. C., M. K. Reedy, K. Leonard, and B. Bullard. 1994. Gold/Fab immunoEM localization of troponin H and troponin T in *Lethocerus* flight muscle. *J. Mol. Biol.* 239:52–67.

Reedy, M. C., M. K. Reedy, and R. T. Tregear. 1988. Two attached non-rigor crossbridge forms in insect flight muscle. *J. Mol. Biol.* 204:357–383.

Reedy, M. K. 1967. Cross-bridges and periods in insect flight muscle. *Am. Zool.* 7:465–481.

Reedy, M. K. 1968. Ultrastructure of insect flight muscle. I. Screw sense and structural grouping in the rigor cross-bridge lattice. *J. Mol. Biol.* 31:155–176.

Reedy, M. K., R. S. Goody, W. Hofmann, and G. Rosenbaum. 1983. Co-ordinated electron microscopy and x-ray studies of glycerinated insect flight muscle. I. X-ray diffraction monitoring during preparation for electron microscopy of muscle fibers fixed in rigor, ATP and AMPPNP. *J. Muscle Res. Cell Motil.* 4:25–53.

Reedy, M. K., K. C. Holmes, and R. T. Tregear. 1965. Induced changes in orientation of the crossbridges of glycerinated insect flight muscle. *Nature.* 207:1276–1280.

Reedy, M. K., K. R. Leonard, R. Freeman, and T. Arad. 1981. Thick myofilament mass determination by electron scattering measurements with the scanning transmission electron microscope. *J. Muscle Res. Cell Motil.* 2:45–64

Reedy, M. K., C. Lucaveche, and D. Popp. 1991. Fixation of insect flight muscle by "TAOS" and "TAURAC" tannic-acid-metal procedures. *Biophys. J.* 59:579*a*. (Abstr.)

Reedy, M. K., C. Lucaveche, M. C. Reedy, and B. Somasundaram. 1993. Experiments on rigor crossbridge action and filament sliding in insect flight muscle. *In* Mechanism of Myofilament Sliding in Muscle Contraction. H. Sugi and G. H. Pollack, editors. Plenum Press, New York. 33–46.

Reedy, M. K., C. Lucaveche, M. C. Reedy, K. A. Taylor, and B. Somasundaram. 1992. Hybrid sarcomeres of insect flight muscle, where rigor overlap zones abut relaxed H-bands. *Biophys. J.* 61:286*a*. (Abstr.)

Reedy, M. K., and M. C. Reedy. 1985. Rigor crossbridge structure in tilted single filament layers and flared-X formations from insect flight muscle. *J. Mol. Biol.* 185:145–176.

Schmitz, H., F. T. Ashton, F. A. Pepe, and G. Beinbrech. 1993. Invertebrate myosin filament: parallel subfilament arrangement in the wall of solid filaments from the honeybee, *Apis mellifica. Tissue & Cell.* 25:457–462.

Schmitz, H., F. T. Ashton, F. A. Pepe, and G. Beinbrech. 1994. Substructures in the core of thick filaments: arrangement and number in relation to the paramyosin content of insect flight muscles. *Tissue & Cell.* 26:83–100.

Squire, J. M. 1972. General model of myosin filament structure. II. Myosin filaments and cross-bridge interactions in vertebrate striated and insect flight muscles. *J. Mol. Biol.* 72:125–138.

Squire, J. M. 1992. Muscle filament lattices and stretch activation: the match-mismatch model reassessed. *J. Muscle Res. Cell Motil.* 13: 183–189.

Squire, J. M., P. K. Luther, and E. P. Morris. 1990. Organization and properties of the striated muscle sarcomere. *In* Molecular Mechanisms in Muscular Contraction. J. M. Squire, editor. Macmillan Press LTD, New York.

Taylor, K. A., and R. A. Crowther. 1991. A protocol for 3-D image reconstruction from a single image of an oblique section. *Ultramicroscopy.* 38:85–103.

Taylor, K. A., M. C. Reedy, L. Córdova, and M. K. Reedy. 1984. Three-dimensional reconstruction of rigor insect flight muscle from tilted thin sections. *Nature.* 310:285–291.

Taylor, K. A., M. C. Reedy, L. Córdova, and M. K. Reedy. 1989a. Three-dimensional image reconstruction of insect flight muscle. I. The rigor myac layer. *J. Cell Biol.* 109:1085–1102.

Taylor, K. A., M. C. Reedy, L. Córdova, and M. K. Reedy. 1989b. Three-dimensional image reconstruction of insect flight muscle. II. The rigor actin layer. *J. Cell Biol.* 109:1103–1123.

Taylor, K. A., M. C. Reedy, M. K. Reedy, and R. A. Crowther. 1993. Crossbridges in the complete unit cell of rigor insect flight muscle imaged by 3-D reconstruction from oblique sections. *J. Mol. Biol.* 233:86–108.

Tregear, R. T., K. Wakabayashi, H. Iwamoto, M. C. Reedy, M. K. Reedy, H. Sugi, and Y. Amemiya. 1990. x-ray diffraction and electron microscopy from *Lethocerus* flight muscle partially relaxed by adenylylimidodiphosphate and ethylene glycol. *J. Mol. Biol.* 214: 129–141.

Winkler, H., and K. A. Taylor. 1994. 3D reconstruction by combining data from sections cut oblique to different unit cell axes. *Ultramicroscopy.* In press.

Wray, J. S. 1979a. Filament geometry and the activation of insect flight muscles. *Nature.* 280:325–326.

Wray, J. S. 1979b. Structure of the backbone in myosin filaments of muscle. *Nature.* 277:37–40.

Wray, J. S., P. Vibert, and C. Cohen. 1979. Actin filaments in muscle: pattern of myosin and tropomyosin/troponin attachments. *J. Mol. Biol.* 124:501–521.